This article has been accepted for publication in a future issue of this journal, but has not been fully edited. Content may change prior to final publication. Citation information: DOI 10.1109/TTHZ.2021.3083939, IEEE Transactions on Terahertz Science and Technology

A 670 GHz Integrated InP HEMT Direct-Detection Receiver for the Tropospheric Water and Cloud Ice (TWICE) Instrument

Caitlyn Cooke *Student Member*, Kevin M. K. H. Leong *Member*, Alexis Zamora *Member*, Ben S. Gorospe, X.B. Mei *Member*, Pekka Kangaslahti *Member*, Erich Schlecht *Member*, Mehmet Ogut *Member*, Yuriy Goncharenko, *Member*, Steven C. Reising *Senior Member*, and William R. Deal *Fellow*

***Abstract*—In this work, a novel 670-GHz integrated direct-detection receiver using 25-nm InP HEMT technology is presented. This is the first demonstration of an integrated direct detection radiometer architecture at these frequencies. The receiver exhibits a noise figure of 11.4 dB with a total DC power consumption of 0.25 W. The integrated receiver measures only 0.8 cm x 1.3 cm x 4.8 cm (0.3” x 0.5” x 1.9”). These results show that transistor-based direct-detection receivers are a viable technology for submillimeter wave applications, with low SWaP with no compromise in performance.**

***Index Terms*—radiometer, low noise amplifier, MMIC, 1/f noise, calibration, HEMT, sub-millimeter wave**

I. Introduction

Ice clouds in the upper atmosphere are a major source of uncertainty in climate models. Global observation of ice particles in the upper troposphere could provide information on the influence of aerosol pollution on ice particle size, which affect cloud precipitation processes and albedo [1-3]. Submillimeter wave radiometric instruments can fill the gap in cloud ice particle size information between approximately 50 µm and 1 mm. For example, CloudSat’s 94 GHz radar observes particles larger than ~600 µm in diameter, and MODIS infrared radiometers observe particles smaller than ~50 µm [2]. The Tropospheric Water and Cloud Ice (TWICE) instrument seeks to perform global observations of ice particle size and water vapor profiles from a 6U CubeSat platform, using 16 submillimeter wave radiometric channels ranging from 118 GHz to 850 GHz [1].

Manuscript received May 22, 2021. This material is based upon work supported by NASA under grant NNX14AK70G.

C. M. Cooke is with the Northrop Grumman Corporation, Redondo Beach, CA 90278 USA, and the Electrical Engineering Department, University of Colorado, Boulder, CO 80309 USA (e-mail: caitlyn.cooke@ngc.com).

K. Leong, A. Zamora, B. Gorospe, X. B. Mei, and W. R. Deal are with the Northrop Grumman Corporation, Redondo Beach, CA 90278 USA (e-mail: kevin.leong@ngc.com; gerry.mei@ngc.com; william.deal@ngc.com).

P. Kangaslahti, E. Schlecht and M. Ogut are with the NASA Jet Propulsion Laboratory, California Institute of Technology, Pasadena, CA 91109 USA (e-mail: pekka.k.kangaslahti@jpl.nasa.gov).

S. C. Reising and Y. Goncharenko are with the Microwave Systems Laboratory, Colorado State University, Fort Collins, CO 80523 USA (e-mail: Steven.Reising@ColoState.edu).

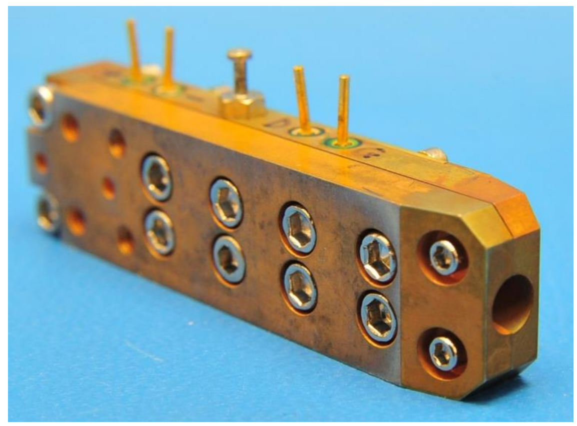

Fig. 1. Photograph of the 670 GHz integrated receiver, with dimensions of 0.8 cm x 1.3 cm x 4.8 cm (0.3” x 0.5” x 1.9”).

The 16-channel TWICE CubeSat instrument is enabled by low SWaP direct-detection integrated receivers using 25-nm InP HEMT transistor amplifiers. Direct-detection receivers consume significantly less power and use fewer components compared to similar heterodyne receivers. This allows them to be integrated into small, lightweight, and low power form factors ideal for CubeSat applications [4-5].

Significant work has already been performed on compact, low DC power radiometric receivers in the high millimeter to submillimeter wave frequency range up to 850 GHz [6-11]. The Tropical Systems Technology Demonstration (TEMPEST-D) satellite mission uses NGC 35-nm InP HEMT direct detection receivers to observe thermal radiation at frequencies from 87 to 181 GHz [12], and the Compact Submillimeter Wave and Long-Wave Infrared (LWIR) Polarimeter (SWIRP) instrument contains 220 GHz and 680 GHz direct detection dual-channel polarimeters leveraging the NGC 25-nm InP HEMT process. The receiver presented in this work is the 670 GHz channel of the TWICE instrument, shown in Fig. 1, which is the most compact and lowest power consumption direct detection receiver at 670 GHz to date. The receiver has demonstrated radiometric resolution improvement in direct detection receivers with a novel 1/f noise mitigation technique [13].

The paper is organized as follows. Section II describes each major component of the receiver including the horn antenna design, the low noise amplifier, the bandpass filter, and the diode detector. Each component was prototyped individually in split-block modules and characterized before designing and fabricating the integrated receiver. Results from the prototypes are provided in each respective component subsection. Section III describes the characterization and performance of the final integrated receiver. This includes noise figure, output voltage, and analysis of receiver radiometric resolution. The measurement of radiometric resolution is performed both with and without the addition of a novel technique to mitigate gain fluctuations from 1/f noise [13].

II. Receiver Architecture

A. Integrated Receiver Overview

The block diagram of the 670 GHz direct-detection receiver is shown in Fig. 2. The 25 nm InP HEMT MMIC LNAs at the front end of the receiver enable the use of the direct-detection architecture. The noise figure of these LNAs is comparable to the conversion loss of GaAs Schottky mixers at the same frequency in heterodyne systems [14]. The elimination of the mixer and LO chain reduces DC power consumption and reduces receiver size and complexity, which makes the direct-detection architecture ideal for CubeSat instruments such as TWICE which require small size, weight and power. The receiver components are integrated into a single split-block housing with dimensions of 0.8 cm x 1.3 cm x 4.8 cm (0.3” x 0.5” x 1.9”). WR-1.5 waveguide connects the internal components, resulting in a compact flangeless form factor.

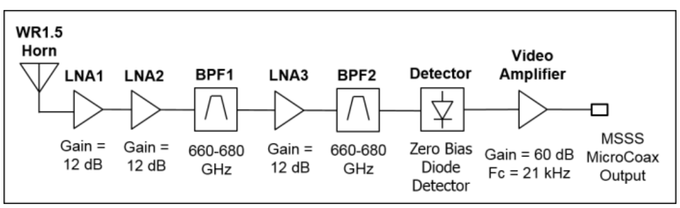

Fig. 2. TWICE 670 GHz integrated receiver block diagram.

Table I provides the detailed specifications for the receiver, including measured capabilities of noise figure, DC power consumption, and RF gain. The center frequency of 670 GHz was chosen to be within an atmospheric window that allows the sensor to provide sensitivity to cloud ice particles of a certain range of sizes. Multiple sensors at a set of frequencies from 240 to 850 GHz in the TWICE instrument are used to provide information on cloud ice particle size in the upper troposphere [2-3].

The direct detection technique enables low DC power consumption. The total receiver DC power consumption is 264 mW, including the LNA bias and video amplifier bias. This is lower than heterodyne receivers at similar frequency ranges by about a factor of 10 [5].

A photograph showing the internal RF path of the receiver is provided in Fig. 3a. The received signal is amplified by two initial LNA stages with a combined gain of approximately 24 dB, including transition losses. The LNAs are fabricated using Northrop Grumman’s 25 nm InP HEMT process, which is described in [15]. A 660-680 GHz waveguide bandpass filter then band limits the spectrum at the output of the second LNA to prevent compression of the third LNA. A second bandpass filter further band limits the spectrum at the output of the third LNA to prevent compression of the detector diode. The signal is detected using a zero bias Schottky diode detector produced by Virginia Diodes, Inc. (VDI).

TABLE I
Specifications for 670 GHz Receiver

Parameter	Quantity	Units
Center Frequency	672.5	GHz
Bandwidth	660-680	GHz
Cascaded Noise Figure	11.4	dB
Ambient Output Voltage	1	V
Total RF Gain	36	dB
DC Power Consumption	264	mW
DC Voltage Inputs	1.2, 2.5, 10, -10	V
Dimensions	0.8 x 1.3 x 4.8	cm
Weight	40	g

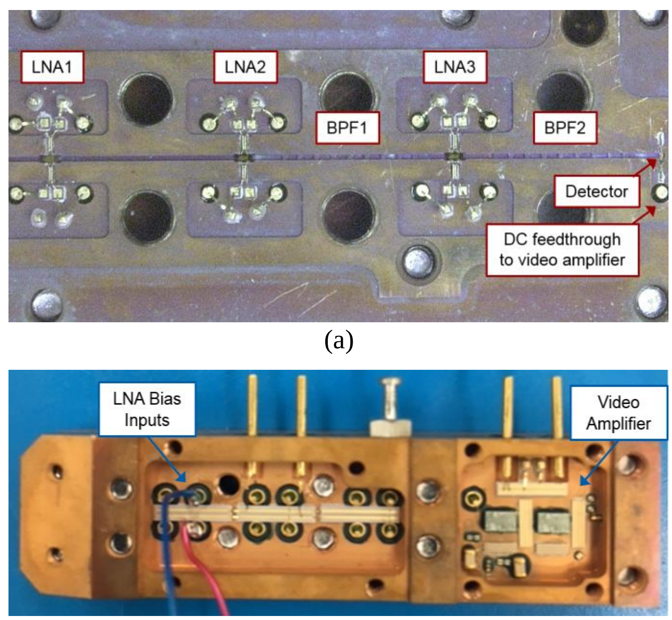

(a)

(b)

Fig. 3. (a) Internal view of the 670 GHz receiver RF path, (b) DC bias cavity with chip and wire video amplifier on the reverse side.

The detector output voltage is amplified using a video amplifier to maximize ADC dynamic range. The detector output is routed by a DC feedthrough to the MIC video amplifier assembled on the back side of the housing, shown in

This article has been accepted for publication in a future issue of this journal, but has not been fully edited. Content may change prior to final publication. Citation information: DOI 10.1109/TTHZ.2021.3083939, IEEE Transactions on Terahertz Science and Technology

Fig. 3b. The LNA DC biasing circuitry is also fed through from the back side of this integrated housing.

B. WR-1.5 Horn

The antenna is a broadband multiflare angle circular horn design, which has been demonstrated up to 1.9 THz in [16]. The multiflare angle horn design has performance characteristics similar to a corrugated horn, including low cross polarization, low side lobe levels, and good beam circularity, but is easier to machine, making the design more repeatable at high frequencies.

Fig. 4 shows the circular horn antenna prototype assembly, as well as the integrated receiver horn machined into the split-block waveguide housing. The antenna is designed with a circular-to-rectangular waveguide transition that is also machined into the split-block assembly.

The simulated versus measured E-plane and H-plane radiation patterns for the prototype horn module are shown in Fig. 5. The measured E-plane beamwidth of the antenna is 7.7 degrees, and the H-plane bandwidth is 8.4 degrees, closely matching the 8.4 degree simulated 3 dB beamwidth in both planes. The calculated directivity of this antenna is 28 dB, calculated from the 3 dB bandwidth. The measured return loss of the antenna is not shown here, but was measured to be greater than 20 dB across the WR-1.5 waveguide band.

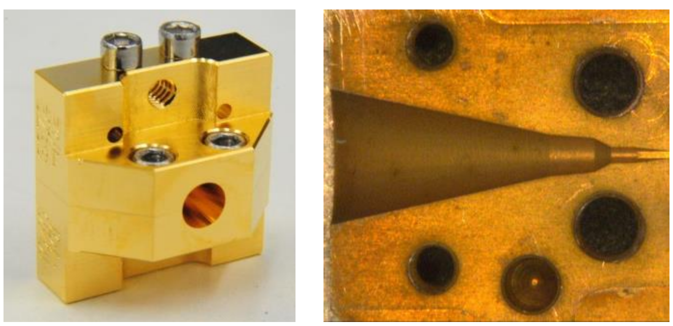

Fig. 4. Prototype horn antenna module (left). Horn antenna with circular to WR-1.5 rectangular waveguide transition machined into the split-block receiver housing (right).

C. LNA Design

The LNA MMIC shown in Fig. 6 consists of eight 12 µm gate periphery transistor stages matched to an intermediate impedance consisting of a series CPW line and shunt DC blocking capacitor. The lengths of the interconnect CPW lines are tuned independently, and each are between 0 and 3 µm in length. The input and output are matched to 50 ohms using open-circuited shunt stubs. Further details regarding the LNA design and HEMT transistor modeling are reported in [14-15].

A CPW-to-coplanar stripline transition connects the input and output 50 Ohm transmission lines of the amplifier to the half-wavelength dipole transitions that couple to the WR-1.5 waveguides. Each dipole transition contributes about 2.5 dB of insertion loss at 670 GHz. Further information on the design and simulation of on-chip dipole transitions can be found in [17].

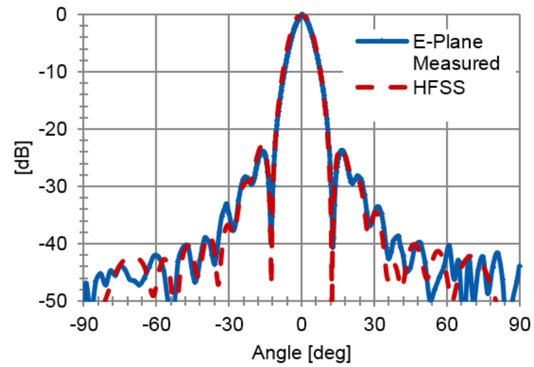

(a)

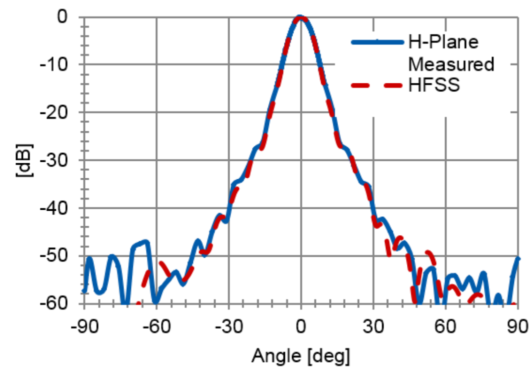

(b)

Fig. 5. Simulated vs. measured (a) E-plane and (b) H-plane cuts of the circular horn radiation pattern.

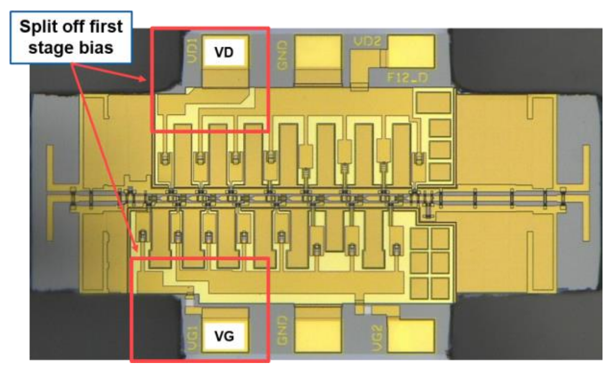

Fig. 6. Photograph of the 670 GHz LNA MMIC with integrated dipole transitions and split-off first transistor bias line for switching to mitigate 1/f noise.

The LNAs were assembled in separate prototype split-block housings, where the gain and noise figure of the LNA have been verified over the frequency range of the 670-GHz receiver. Scattering parameter data from a single packaged prototype is shown in Fig. 7. As seen from Fig. 7, the LNA stage has about 12 dB of gain in package. The packaged noise figure was also measured using the Y-factor method, and was found to be 9.6 dB at 670 GHz, with a maximum of 10.1 dB over the 660 to 680 GHz bandwidth. It should be noted that these measurements are referenced to the waveguide flange interface and therefore include all transition and waveguide losses.

This article has been accepted for publication in a future issue of this journal, but has not been fully edited. Content may change prior to final publication. Citation information: DOI 10.1109/TTHZ.2021.3083939, IEEE Transactions on Terahertz Science and Technology

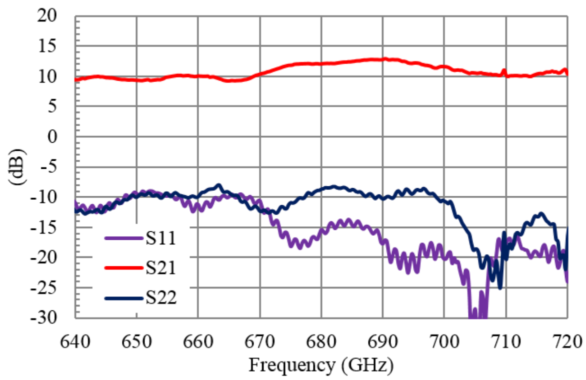

Fig. 7. Scattering parameters of a single packaged prototype LNA. The LNA has a maximum gain of 12 dB and maximum noise figure of 10.1 dB (not shown here) across the 660 to 680 GHz bandwidth.

Compared to [14], a key architectural change has been made. In [14], the bias lines for all gates and drains were tied together at a single gate and drain bias pad. This scheme is quite simple, but requires that all stages are biased equally. For this work, we separate the gate and drain bias for the first stage so that they can be biased independently from the subsequent stages. In the development stage, this was done as a risk mitigation technique to potentially minimize the impact of 1/f noise. It was found during development that 1/f noise did significantly impact performance of the receiver. This technique is further discussed in the subsequent paragraphs.

It is well known that 1/f noise can contribute to receiver NEDT. This is particularly true in direct detection receivers which directly convert RF energy to 0 Hertz. In real semiconductor devices, 1/f noise is follows a linear dependence. This well-behaved 1/f roll-off characteristic intersects with the white noise at the 1/f noise corner frequency. Below the 1/f noise corner frequency, 1/f noise will degrade NEDT. Above this frequency, the impact of 1/f noise on NEDT is minimal. This impact has been demonstrated in [18]. The traditional method for mitigating 1/f noise in direct detection receivers is the Dicke-switched receiver, which toggles between the antenna port and a fixed port impedance at a known physical temperature. Unfortunately, Dicke-switched receivers degrade receiver NEDT both due to the excess insertion loss associated with the switch, but also due to the fact that the antenna is only viewed for half of the time, resulting in a square-root of 2 increase in NEDT, with respect to that of a balanced total-power radiometer.

In this work, we propose an alternate technique for reducing 1/f noise. Instead of switching between the antenna and a known load, as is done in a Dicke-switched receiver, we propose to toggle the bias of the first stage on and off. Since the direct detection receiver consists of a total of 24 amplification stages and one detection stage, we assume that toggling the bias of the first stage may be sufficient to remove the 1/f noise contribution of the remaining 23 transistors and detector diode. This idea was first discussed between Dr. Deal and Dr. Grossman [19]

In this case, the first transistor in the amplifier chain creates an independent reference in the off state that tracks the gain fluctuations due to 1/f noise generated by the low noise amplifiers. While the physical impedance in the off-state is not well known, we postulate that we can numerically relate the residual 1/f noise of the chain to the 1/f noise of the total receiver chain, and then numerically remove the 1/f noise [13]. Fig. 8 shows an example of a toggled control signal and output voltage of the 670 GHz receiver. Each transistor has about 1-2 dB of gain per stage at 670 GHz, so turning off one transistor still produces an appreciable output voltage signal that can be accurately measured by the instrument ADC, and used to create a correction for the signal from the antenna in the first transistor's "on" state.

The 1 kHz switching frequency is chosen to be faster than the 1/f noise corner frequency, but as slow as is reasonable to reduce the total amount of time that the output voltage is spending transitioning from state-to-state. This rise and fall time is limited by the cutoff RC constant of the video amplifier, which sets the video cutoff frequency. Fig. 8 shows a 25 µsec rise time, which represents 5% of the total "on" state measurement time. This sufficiently short transition time reduces the total time the instrument spends observing the cloud target, which in turn reduces the receiver radiometric resolution, so it is important to choose the cutoff frequency of the video amplifier carefully to minimize this transition time as much as possible. The 50% time spent in the reference state also increases the receiver radiometric resolution by the square-root of 2, by reducing the target dwell time. Further discussion of the 1/f noise sensitivity evaluation will be provided in Section III.

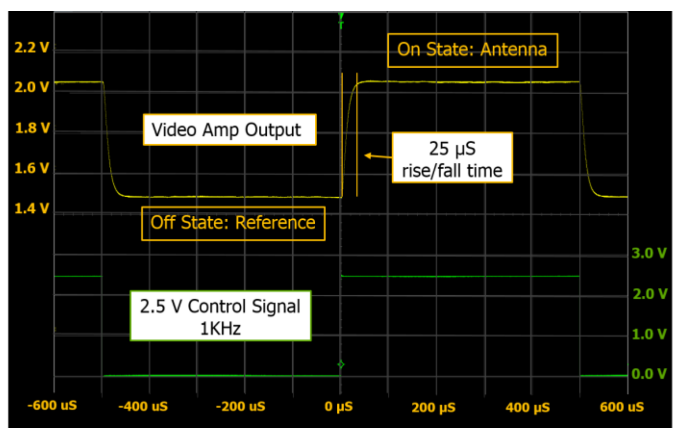

Fig. 8. The output voltage of the receiver vs. time using the 1/f noise reduction technique. The top trace in yellow shows the switched output voltage. The bottom trace in green shows the control signal toggling the gate and drain bias voltage of the first transistor.

To facilitate the toggled bias scheme, we apply the bias between two separate bias pins. The first stage is biased from an applied voltage of 2.5 V amplitude switching at 1 kHz. The 2.5 V amplitude switching voltage was chosen as a convenient value for the output of the TWICE instrument FPGA. Both the gate and drain biases of the first transistor are connected to this switching voltage. All subsequent stages are biased at 1.2 V. The 1.2 V input is set using a series of resistor dividers to the individual MMIC gates. The gate voltages are set so that the MMICs operate at a 400 mA/mm drain current density.

Fig. 9 shows one LNA MMIC packaged in the TWICE receiver split-block housing with DC bias peripherals. The first amplifier MMIC is shown, so the left side DC bias pins bring in the switching signal to bias the first transistor, while the right side DC bias pins bring in a constant voltage to bias subsequent transistors. The MMIC DC bias pads are wirebonded to a 3-mil thick quartz substrate, which is wirebonded to a 100 pF single-layer capacitor. The DC feedthroughs connect to the resistor divider networks on the back side of the receiver.

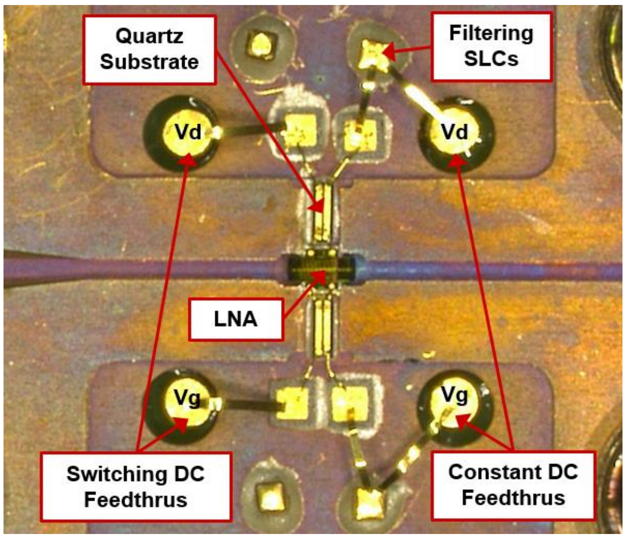

Fig. 9. Assembled LNA MMIC packaged in the integrated TWICE housing with DC bias peripherals.

D. Bandpass Filter Design

Two identical bandpass filters are machined into the integrated split-block receiver housing. Each one is an 8-pole waveguide iris filter. Fig. 10 shows a photograph of the lower half of the filter machined into the receiver housing, along with a CAD model of the complete filter shape. The total length of the iris filter is approximately 1 cm.

The filter is designed using a hybrid simulation method that allows for rapid optimization. A single iris section is simulated using Ansys HFSS by varying iris thickness. Once the HFSS simulations are completed, the resulting simulation files are cascaded in Keysight ADS. This allows us to efficiently optimize both iris thickness and length between filter sections. The full filter design is then transferred back into HFSS for verification.

Several prototype filter iterations were fabricated to better understand the effects of machining tolerances on the filter performance. This is especially important when examining filters for the integrated receiver design, since the two filters within the housing cannot be evaluated individually. Two prototype filter iterations were designed before the integrated receiver housing was finalized. Simulated versus measured results of the bandpass spectral responses are shown in Fig. 11.

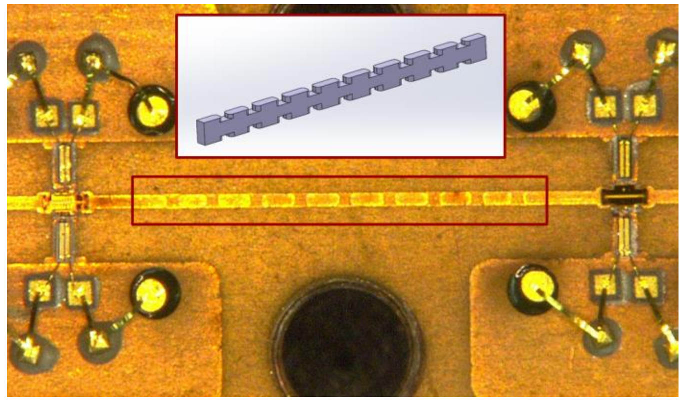

Fig. 10. Photograph of the split-block machined waveguide iris bandpass filter, and full CAD model.

A significant downward frequency shift was observed in the measurements of the first iteration of filters, as shown in Fig. 11a. The average center frequency is 640 GHz, which is a 5% downward shift from the designed 672 GHz center frequency. The overall bandwidth of each filter is also about 5 GHz wider than simulated. This shift in performance is attributed to systematic machining variations. The measured insertion loss is 3-4 dB, compared to the simulated 2 dB insertion loss.

The second iteration of filters was purposefully designed to be higher in frequency than the desired model to compensate for the downward frequency shift observed in the first iteration. The upward frequency shift is obtained by reducing the length of the thicker capacitive filter sections. The measured results from the second iteration are shown in Fig. 11b. The average center frequency is shifted upward by about 3%, and shows about 10 GHz of variation among the filter samples measured.

A tuning method was employed to shift the filters to the desired frequency range centered at 672 GHz as described in [20]. A small section of ribbon bond wire is added along the length of the filter between the split-block halves, which slightly increases the waveguide dimensions and tunes the filter response downward in frequency. The length and thickness of the individual tuning bond wires are varied for each filter response. If the filter response needs to be shifted upward, the pressure ridges of the waveguide can be carefully sanded to reduce the height of the waveguide. This is not a preferred tuning method, since material is permanently removed from the module. This is why it is preferable to design the filters purposefully higher in frequency and shift them downward with an easily removable and reconfigurable bond wire. Fig. 11c shows that this technique was successfully implemented to tune the iris filters individually to achieve the desired frequency range. In the integrated housing, this method could also be employed on both filters inside the module if the measured center frequency of the receiver significantly deviated from that of the design.

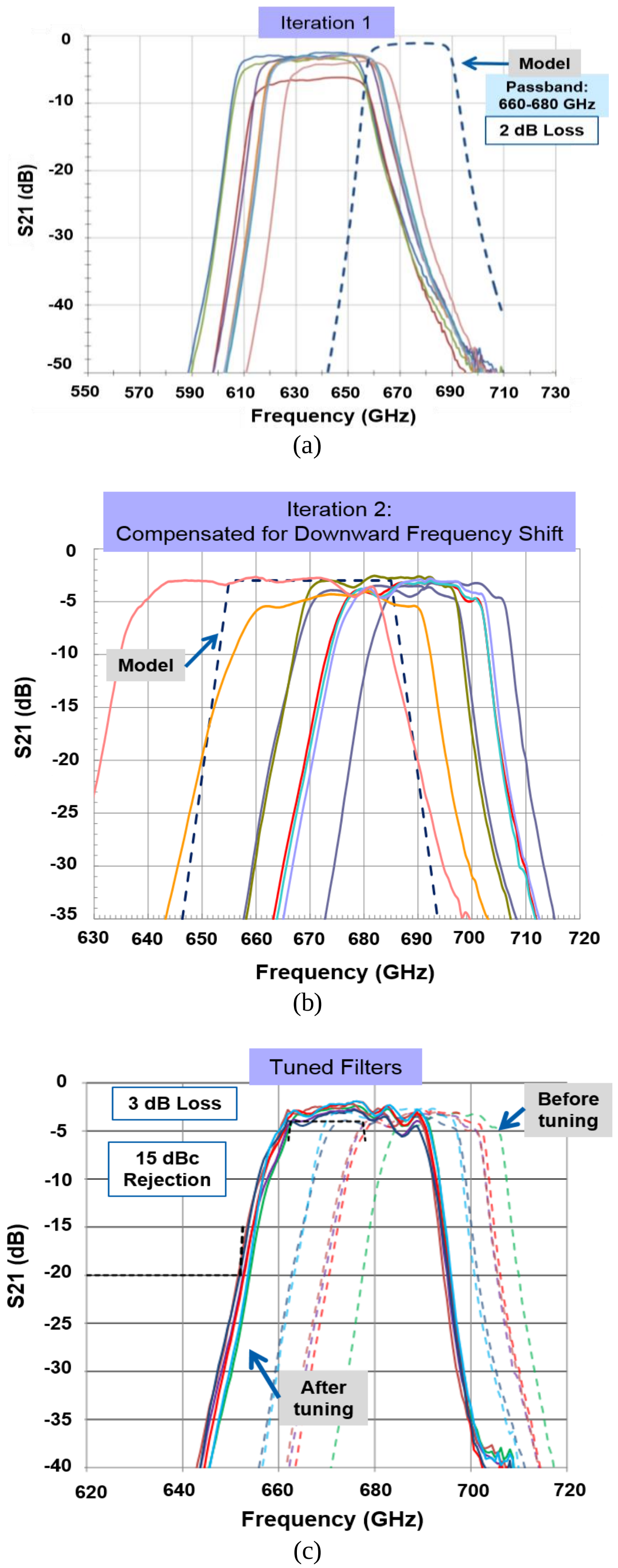

Fig. 11. Modeled versus measured bandpass spectra of the 670 GHz waveguide iris filter prototypes. (a) Iteration 1 with downward frequency shift. (b) Iteration 2 designed purposefully to be higher in frequency to compensate for downshift seen in Iteration 1. (c) Measured response of ribbon-tuned Iteration 2 filters compared to original measured response.

E. Detector and Video Circuit

The detector is a zero-bias Schottky diode detector developed by VDI. A photograph of the diode mounted on a silicon substrate is shown in Fig. 12. A zero bias Schottky diode is mounted on a quartz substrate and printed with an electromagnetic probe that couples to the WR-1.5 waveguide. The output of the detector is wirebonded to a DC feedthrough that connects to the MIC video amplifier on the back side of the receiver. The detector circuit was designed and fabricated by VDI.

The detector substrates were also tested prior to integration into the TWICE receiver housing using a stand-alone split-block test fixture. A Virginia Diodes amplified multiplier chain frequency source was used to input a signal of approximately -30 dBm into the split-block housing, and the responsivity of the diode detector was measured over frequency. From the measured results shown in Fig. 13, the responsivity is greater than 1000 mV/mW in the 660 to 680 GHz operating range.

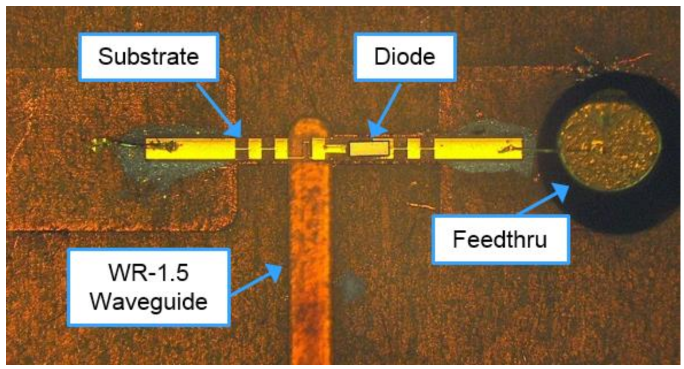

Fig. 12. Photograph of the zero-bias Schottky diode detector mounted in the receiver housing. The diode is attached to a 2 mil thick silicon substrate printed with a receiving antenna and matching network.

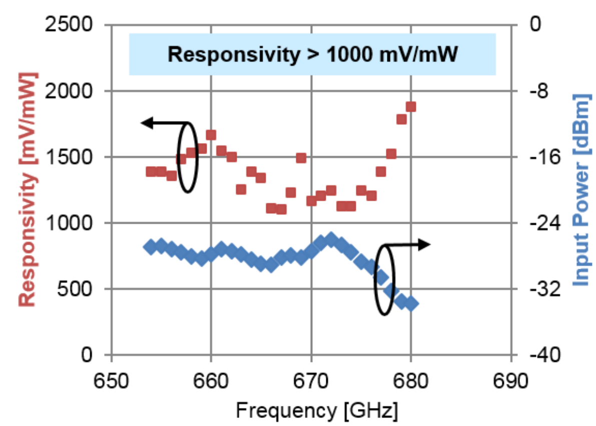

Fig. 13. Measured responsivity of the diode detector as a function of frequency, shown along with input power.

The video amplifier circuit consists of two cascaded operational amplifiers, providing a total of about 60 dB of gain, with a lowpass cutoff frequency of 21 kHz. Fig. 14 shows the video amplifier circuit implemented with bare die

This article has been accepted for publication in a future issue of this journal, but has not been fully edited. Content may change prior to final publication. Citation information: DOI 10.1109/TTHZ.2021.3083939, IEEE Transactions on Terahertz Science and Technology

connected with wirebonds, allowing the circuit to fit into a smaller form factor. The video amplifier IC is a bare die OP27 manufactured by Analog Devices. The external pins supply +/-10 V bias to the video amplifier. The total power consumption of the video amplifier is 120 mW, accounting for about half of the power consumption of the integrated receiver.

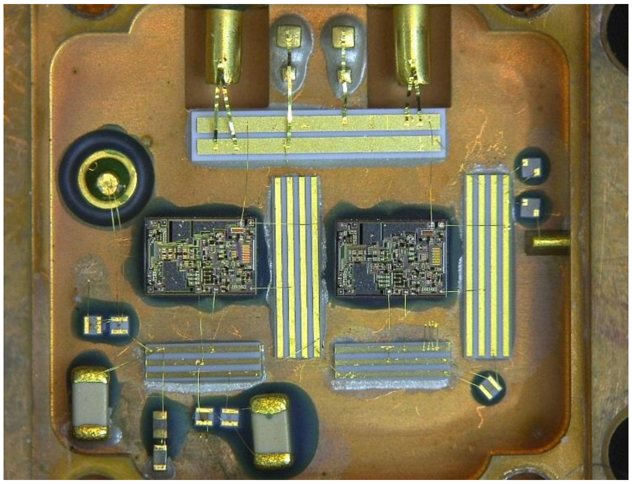

Fig. 14. Photograph of the chip and wire video amplifier circuit, mounted on the back side of the 670 GHz receiver.

III. RECEIVER PERFORMANCE

A. *Receiver Integration Method*

The integrated receiver is first populated with passive CPW transmission line ICs with dipole transitions in place of the three LNAs. This allows measurement of the filter's frequency response independently from the LNA response and possible process variations. It also verifies the functionality of the detector without complicating the debugging process with multiple active components in the chain. Fig. 15 shows the test setup for this measurement. The receiver is excited with a VDI WR-1.5 amplified multiplier chain. This allows the source frequency to be varied across the filter bandwidth and excited with enough signal strength to be read by the detector without the LNA gain.

The source and the device under test (DUT) are placed about 7.5 cm (3”) apart so that the signal level is strong enough at the detector to achieve adequate dynamic range without LNAs. The source power is calibrated by placing a test horn antenna as input to an Erickson PM5 power meter and measuring the source power at the same 7.5 cm (3”) distance.

Fig. 16 shows the measured normalized frequency response of the integrated receiver populated with dipole through-lines in the place of the LNAs. The measured bandwidth of the module is seen to be 24 GHz. The center frequency of the module is shifted downward to 662 GHz, which represents a modest 1.5% shift in frequency. This frequency range was determined to still meet science goals, so no further action was taken to tune this filter using the sanding methods discussed in Section II.

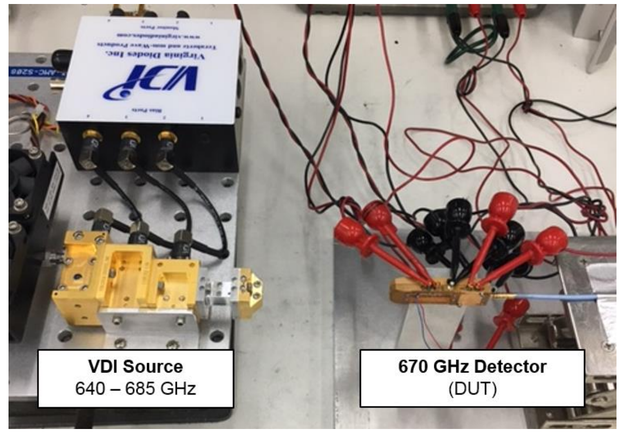

Fig. 15. Test setup for the filter shape and detector functionality measurements using a VDI WR-1.5 active multiplier chain source to sweep an input signal to the receiver over bandwidth.

The through-lines in the receiver were replaced one-by-one, and the measurement was repeated using a similar setup. The distance between the source and DUT was recalibrated as each LNA was added to avoid compressing the detector as gain stages were added. After all MMIC amplifiers were populated, the receiver was aimed at an ambient submillimeter-wave absorber to measure the output voltage of the receiver when measuring ambient noise. The output voltage level is desired to be 1-2 V, which allows the signal to be measured with adequate dynamic range using the TWICE instrument ADC. The output voltage of this receiver is 1.6 V when measuring an ambient submillimeter-wave absorber, verifying that all three amplifier stages provide adequate gain.

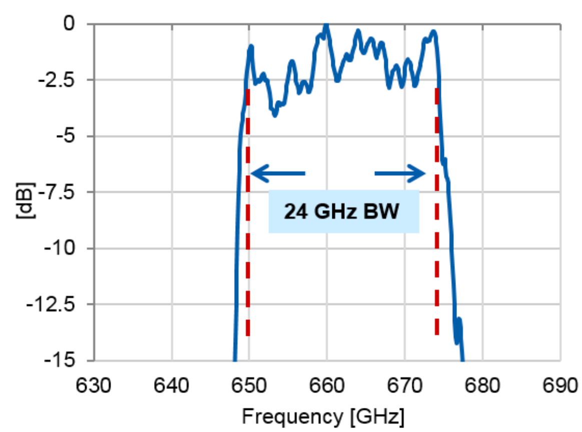

Fig. 16. Normalized frequency response of one integrated receiver prototype populated with bandpass filters and through-lines. The bandwidth is measured to be 24 GHz, with a downward-shifted center frequency of 662 GHz.

B. Noise Figure

The receiver noise figure is measured using the Y-factor method with the test setup shown in Fig. 17. The receiver is placed in front of a small opening in the plexiglass enclosure. An absorber is attached to a heated chopper wheel, which cycles between the hot target and a liquid nitrogen (LN_2) cooled absorber behind it. The noise figure measured using this setup is 11.4 dB. This measurement is the noise figure integrated over the entire 24 GHz receiver bandwidth.

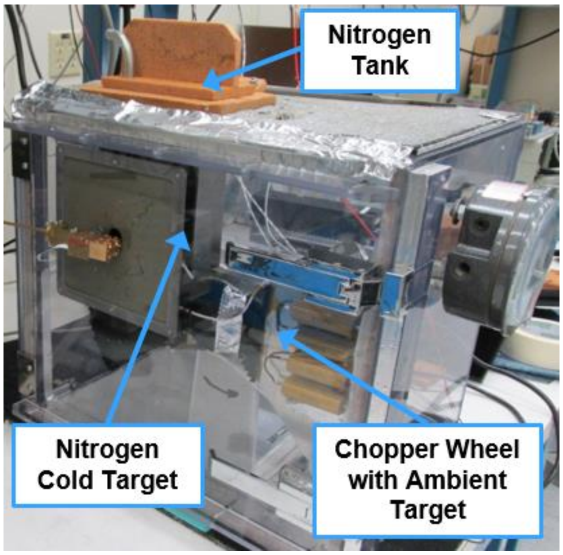

Fig. 17. Y-factor heterodyne noise figure test set.

C. TWICE Instrument Parameters

The operating parameters of the TWICE instrument are integral in evaluating the radiometric performance of the receivers. This section defines the end user requirements for the TWICE instrument, which help to define success criteria for the receiver performance.

The NEDT requirement for the TWICE instrument is determined from the intended application to provide cloud ice particle size information at multiple submillimeter wave frequencies from 240 to 850 GHz. Based on simulations of atmospheric remote sensing retrievals, the required NEDT of the 670-GHz receiver is 1 K [3].

Since the TWICE instrument performs end-to-end calibration with two known references every second, instrument temperature variations can be effectively removed. A very similar calibration technique has been successfully demonstrated on-orbit by the calibration and validation of TEMPEST-D [21]. Results demonstrated that the TEMPEST-D CubeSat instrument is a very well-calibrated, low-noise and highly stable radiometer, rivaling that of much larger operational instruments [21].

The frequency response of the measurement is accounted for during calibration, i.e. when converting the measured power to a brightness temperature through the effective bandwidth of the radiometer. The suitability of the brightness temperature measurements for use in atmospheric remote sensing retrievals does not depend strongly on the frequency response, as long as it is stable.

In the TWICE instrument, two calibration sources, i.e. cosmic microwave background and an ambient blackbody calibration target, are measured every second, and the Earth target is measured in between the two calibration sources [1].

D. 1/f Noise Stability

The stability and accuracy of the 670 GHz receiver are critical for the reliability of radiometric measurements. The stochastic noise properties of the 670 GHz receiver (e.g., 1/f noise performance) are crucial to determine the receiver performance. For stability testing, the designed TWICE command and data handling (C&DH) and power regulation subsystems have been operated with the integrated 670 GHz radiometer [22]. During the test, the C&DH boards performed digital acquisition of the 670 GHz radiometric data while the receiver measured an ambient calibration target at constant room temperature. The frequency spectrum of the radiometric measurements during the stability test is provided in Fig. 18 labeled as "without 1/f noise correction". The initial test results indicated that high 1/f noise in the system dominates the performance of the radiometer. It has been shown in [18] that 1/f noise stability of the 670 GHz InP HEMT low-noise amplifiers has been successfully measured with a zero-bias Schottky detector diode. For the integrated 670 GHz direct detection receiver under test, the three MMICs and the GaAs zero-bias diode contribute to the cumulative 1/f noise response.

The LNA switching technique described in Section II.C has been designed to mitigate 1/f noise in the 670 GHz radiometric measurements. The technique is based on controlling the first transistor stage of the first LNA MMIC of the 670 GHz receiver from the Field Programmable Gate Array (FPGA) on the C&DH board. The LNA switching technique generates two different gain stages of the radiometric measurements that can be designated "antenna" and "reference" for the LNA ON and OFF states, respectively. The switching rate is chosen to be high enough to track the 1/f noise gain variations in the system. The correction in the digitized samples has been applied by comparing the gain variations in both LNA ON and OFF states of measurement.

The power spectral analysis of the TWICE 670 GHz radiometric instrument with 1/f noise correction applied is shown in Fig. 18 labeled as "with 1/f noise correction". As shown in the plotted curves in Fig. 18, the 1/f noise mitigation technique significantly reduces the 1/f noise effect from the radiometric measurements by 19 dB. The corrected 1/f noise curve has a 1/f corner frequency of approximately 1 Hz.

At 670 GHz, the tradeoff in integration time discussed in Section II.C has proven to be less of a detriment for radiometric resolution than the degradation caused by gain fluctuations due to the transistor and Schottky diode 1/f noise contributions. Radiometric measurements were performed

This article has been accepted for publication in a future issue of this journal, but has not been fully edited. Content may change prior to final publication. Citation information: DOI 10.1109/TTHZ.2021.3083939, IEEE Transactions on Terahertz Science and Technology

using a 50 msec integration time. The NEDT of the receiver without the switching technique was measured to be 4.75 K. With the switching technique employed, the NEDT decreased to 0.88 K. This is over 80% improvement in radiometric resolution, which is critical to performing useful measurements to estimate cloud ice particle sizes for atmospheric science. Further details on the test setup and discussion of the results of this method can be found in [13].

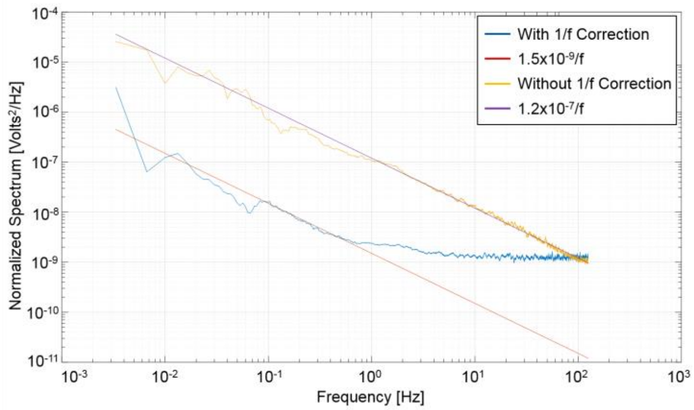

Fig. 18. The normalized PSD response of radiometric receiver with and without the switching method applied.

The improvement in NEDT due to the switching technique meets the specifications of <1 K, as determined by the simulations of atmospheric remote sensing retrievals [3]. This value can still be improved upon in future applications. Using the theoretically ideal equation for NEDT, assuming an ideally flat 24 GHz bandwidth, an integration time of 50 msec, a noise figure of 11.4 dB, and the modulation degradation (50% duty cycle with an additional 5% reduction in integration time due to the rise/fall time), the NEDT would be approximately 0.17 K.

The additional 0.71 K of NEDT is attributed to a number of factors. First, the noise contribution from the first transistor, the one being switched, is not removed. If we approximate that all semiconductor devices contribute as equal additive noise contributors, each transistor contributes 0.18 K of noise (25 devices). Secondly, the filter bandwidth is not perfectly flat. The effective bandwidth is closer to 17.4 GHz, based on the data shown in Fig. 16. Finally, the calibration frequency is 1 Hz. As shown in Fig. 18, there is still some residual spectral noise in the measurement since the calibration frequency is not high enough to be sufficiently above the knee frequency. A faster calibration speed would mitigate this further but would not meet instrument requirements. Finally, there may be some additive 1/f noise from the video amplifier due to low video amplifier drive level. This can be mitigated in the future by either increasing the detector drive level, or choosing a video amplifier with improved 1/f noise at low drive levels.

IV. Conclusions

In this work, a novel 670 GHz integrated direct-detection receiver is presented. The receiver demonstrates a single-sideband noise figure of 11.4 dB integrated over a 24 GHz bandwidth. A filter tuning method is presented to adjust the bandwidth of submillimeter-wave waveguide iris filters, which are highly susceptible to performance shifts due to machining tolerances and plating variations.

The receiver measures only 0.8 cm x 1.3 cm x 4.8 cm (0.3" x 0.5" x 1.9") in size and consumes only 250 mW of DC power. This receiver represents the most compact and lowest power consumption 670 GHz receiver to date, which will further the capabilities of cloud remote sensing instruments. This particular receiver has been integrated into the TWICE instrument as part of a 16-channel radiometer to provide measurements of atmospheric humidity, temperature and cloud ice properties.

The 1/f noise mitigation technique described here produces a 19 dB improvement in stability of the receiver and reduces the NEDT of the receiver to less than 1 K at 670 GHz. Therefore, the presented InP HEMT based receiver exhibits superior noise performance compared to GaAs Schottky receivers up to at least 670 GHz. This is a significant result, demonstrating the viability and superior performance of direct-detection receivers at submillimeter-wave frequencies.

V. Acknowledgements

The authors would like to thank Virginia Diodes, Inc. for their work in providing the diode detector components. This material is based upon work supported by NASA under award number NNX14AK70G, led by Colorado State University. Any opinions, findings, and conclusions or recommendations expressed in this material are those of the author(s) and do not necessarily reflect the views of the National Aeronautics and Space Administration.

References

[1] S. C. Reising, P. Kangaslahti, E. Schlecht, J. Jiang, X. Bosch-Lluis, M. Ogut, Y. Goncharenko, S. Padmanabhan, R. Cofield, N. Chahat, S. T. Brown, W. Deal, A. Zamora, K. Leong, S. Shih and G. Mei, "Tropospheric Water and Cloud ICE (TWICE) Millimeter and Submillimeter-wave Radiometer Instrument for 6U-Class Nanosatellites," In: *Proc. 41st International Conf. on Infrared, Millimeter and Terahertz Waves*, Copenhagen, Denmark, Sept. 2016.

[2] J. H. Jiang, Q. Yue, H. Su, S. C. Reising, P. P. Kangaslahti, W. R. Deal, E. T. Schlecht, L. Wu, and K. F. Evans, "A Simulation of Ice Cloud Particle Size, Humidity, and Temperature Measurements from the TWICE CubeSat," *Earth and Space Science*, vol. 4, no. 8, Jul. 2017. doi:10.1002/2017EA000296.

[3] J. H. Jiang, Q. Yue, H. Su, P. Kangaslahti, M. Lebsock, S. Reising, M. Schoeberl, L. Wu, and R. Herman, "Simulation of Remote Sensing of Clouds and Humidity from Space using a Combined Platform of Radar and Multi-frequency Microwave Radiometers," *Earth and Space Science*, vol. 6, no. 7, Jun. 2019.

[4] W. R. Deal, K. Leong, A. Zamora, W. Yoshida, M. Lange, B. Gorospe, K. Nguyen, and X. B. Mei, "A Low-Power 670-GHz InP HEMT Receiver," *IEEE Transactions on Terahertz Science and Technology*, vol. 6, no. 6, pp. 862-864, Nov. 2016.

[5] E. W. Bryerton, J. L. Hesler, D. Koller, Y. N. Duan and T. W. Crowe, "A Compact Integrated 675–693 GHz Polarimeter," *2018 43rd International Conference on Infrared, Millimeter, and Terahertz Waves (IRMMW-THz)*, Nagoya, Japan, 2018, pp. 1-2.

This article has been accepted for publication in a future issue of this journal, but has not been fully edited. Content may change prior to final publication. Citation information: DOI 10.1109/TTHZ.2021.3083939, IEEE Transactions on Terahertz Science and Technology

[6] S. C. Reising, P. Kangaslahti, S. T. Brown, D. E. Dawson, A. Lee, D. Albers, O. Montes, T. C. Gaier, D. J. Hoppe, and B. Khayatian, "InP HEMT low-noise amplifier-based millimeter-wave radiometers from 90 to 180 GHz with internal calibration for remote sensing of atmospheric wet-path delay," *2012 IEEE/MTT-S International Microwave Symposium Digest*, Montreal, Quebec, Canada, 2012, pp. 1-3.

[7] S. Padmanabhan, T. C. Gaier, B. H. Lim, R. Stachnik, A. Tanner, S. Brown, S. C. Reising, W. Berg, C. D. Kummerow, and V. Chandrasekar, "Radiometer for the Temporal Experiment for Storms and Tropical Systems Technology Demonstration Mission," *Proc. 2018 IEEE International Geoscience and Remote Sensing Symposium (IGARSS)*, Valencia, Spain, 2018, pp. 2001-2003.

[8] P. Kangaslahti, E. Schlecht, J. Jiang, W. R. Deal, A. Zamora, K. Leong, S. C. Reising, X. Bosch, and M. Ogut, "CubeSat scale receivers for measurement of ice in clouds," *2016 14th Specialist Meeting on Microwave Radiometry and Remote Sensing of the Environment (MicroRad)*, Espoo, Finland, 2016, pp. 42-47.

[9] C. M. Cooke, K. M. K. H. Leong, A. Escorcia, K. Nguyen, X. B. Mei, J. Arroyo, T. W. Barton, D. L. Wu, and W. R. Deal, "A 220-GHz InP HEMT Direct Detection Polarimeter," *IEEE Trans. on Microwave Theory and Techniques*, vol. 67, no. 12, pp. 5191-5201, Dec. 2019.

[10] D. L. Wu, “SWIRP: Compact Submm-wave and LWIR Polarimeters for Cirrus Ice Properties,” presented at the NASA Earth Science Technology Forum, Mountain View, CA, USA, Jun. 11-13, 2019.

[11] K. M. K. H. Leong, X. B. Mei, W. H. Yoshida, A. Zamora, J. G. Padilla, B. S. Gorospe, K. Nguyen, and W. R. Deal, "850 GHz Receiver and Transmitter Front-Ends Using InP HEMT," *IEEE Trans. on Terahertz Science and Technology*, vol. 7, no. 4, pp. 466-475, July 2017.

[12] S. Padmanabhan, T. C. Gaier, A. B. Tanner, S. T. Brown, S. C. Reising, B. H. Lim, R. Stachnik, R. Bendig and R. Cofield, "TEMPEST-D Radiometer: Instrument Description and Pre-Launch Calibration," *IEEE Transactions on Geoscience and Remote Sensing*, accepted with minor revisions, Jul. 2020.

[13] M. Ogut, C. Cooke, W. Deal, P. Kangaslahti, A. Tanner, and S. C. Reising, "A Novel 1/f Noise Mitigation Technique Applied to a 670 GHz Receiver, " *IEEE Transactions on Terahertz Science and Technology*, in press, Oct. 2020.

[14] W. R. Deal, A. Zamora, K. Leong, P. H. Liu, W. Yoshida, J. Zhou, M. Lange, B. Gorospe, K. Nguyen, and X. B. Mei, "A 670 GHz Low Noise Amplifier with <10 dB Packaged Noise Figure," *IEEE Microwave and Wireless Components Letters*, vol. 26, no. 10, pp. 837-839, Oct. 2016.

[15] X. Mei, W. Yoshida, M. Lange, J. Lee, J. Zhou, P. H. Liu, K. Leong, K. Leong, A. Zamora, J. Padilla, S. Sarkozy, R. Lai, and W. R. Deal, "First Demonstration of Amplification at 1 THz Using 25-nm InP High Electron Mobility Transistor Process," *IEEE Electron Device Lett.*, vol. 36, no. 4, pp. 327-329, April 2015.

[16] N. Chahat, T. J. Reck, C. Jung-Kubiak, T. Nguyen, R. Sauleau and G. Chattopadhyay, "1.9-THz Multiflare Angle Horn Optimization for Space Instruments," *IEEE Transactions on Terahertz Science and Technology*, vol. 5, no. 6, pp. 914-921, Nov. 2015.

[17] K. M. K. H. Leong, W. R. Deal, V. Radisic, X. B. Mei, J. Uyeda, L. Samoska, A. Fung, T. Gaier, and R. Lai, "A 340–380 GHz Integrated CB-CPW-to-Waveguide Transition for Sub Millimeter-Wave MMIC Packaging," *IEEE Microwave and Wireless Components Lett.*, vol. 19, no. 6, pp. 413-415, June 2009.

[18] E. N. Grossman, K. Leong, X. Mei and W. Deal, "Low-Frequency Noise and Passive Imaging With 670 GHz HEMT Low-Noise Amplifiers," *IEEE Transactions on Terahertz Science and Technology*, vol. 4, no. 6, pp. 749-752, Nov. 2014.

[19] E-Mail correspondence between Dr. Bill Deal and Dr. Erich Grossmann, 2014.

[20] S. E. Shih, B. Gorospe, K. Leong, and W. R. Deal, “Terahertz filter tuning,” U.S. Patent 9,947,980, 2018.

[21] W. Berg, S. T. Brown, B. H. Lim, S. C. Reising, Y. Goncharenko, C. D. Kummerow, T. C. Gaier and S. Padmanabhan, "Calibration and Validation of the TEMPEST-D CubeSat Radiometer, " *IEEE Transactions on Geoscience and Remote Sensing*, early release online, Sept. 2020.

[22] M. Ogut, S. C. Reising, X. Bosch-Lluis, Y. V. Goncharenko, B. Kilmer, P. Kangaslahti, E. Schlecht, R. Cofield, A. Skalare, S. Padmanabhan, J. Jiang, S. T. Brown, W. R. Deal and A. Zamora, "Design, Testing and Reliability Analysis of Command and Data Handling (C&DH) Subsystem for the Tropospheric Water and Cloud Ice (TWICE) Instrument for a 6U-Class Small Satellite," *Proc. 2018 IEEE International Geoscience and Remote Sensing Symposium (IGARSS)*, Valencia, Spain, Jul. 2018, pp. 1990-1993.

Caitlyn M. Cooke (S’16) received the B.S. and M.S. degrees in electrical engineering both from the University of Colorado at Boulder, Boulder, CO, USA, in 2014 and 2016, respectively, and is currently working toward the Ph.D. degree in electrical engineering at the University of Colorado at Boulder.

From 2014 to 2017, she was with NASA Goddard Space Flight Center, Greenbelt, MD, USA, involved with submillimeter-wave radiometers for CubeSats. She received the NASA Space Technology Research Fellowship in 2016, for research on millimeter-wave monolithic microwave integrated circuits for radiometer front-ends. She currently an RF Design Engineer at Northrop Grumman Aerospace Systems, Redondo Beach, CA, USA, where she is focused on high frequency MMIC design and packaging.

Kevin M. K. H. Leong (M’04) received the B. S. degree in electrical engineering from the University of Hawaii at Manoa in 1999 and the M. S. degree and Ph.D. in electrical engineering from the University of California at Los Angeles in 2001 and 2004, respectively. Dr. Leong was awarded the Microwave Prize at the Asia Pacific Microwave Conference in 2006. From 2004 to 2007, he was a postdoctoral researcher at UCLA. Currently, he is a staff engineer at Northrop Grumman Aerospace Systems, Redondo Beach, CA, where he is involved in high frequency MMIC and package design.

Alexis Zamora earned his B.S. and M.S. degrees in electrical engineering from the University of Hawaii at Manoa in 2008 and 2010, respectively. In 2011 he joined Northrop Grumman Aerospace Systems, Redondo Beach, CA, where he predominantly does MMIC design on various III-V technologies. In 2017 he became a section manager in the Radio Frequency-Mixed Signal department. His main area of interest is InP-HEMT-based high frequency electronics. Mr. Zamora was awarded the 2016 IEEE EDL “George E. Smith” Best Paper Award.

Ben S. Gorospe received technician diploma from DeVry Institute of Technology in Phoenix in 1982. He joined TRW now Northrop Grumman Aerospace Systems in 1982 where he works on assembly and test of RF electronics. Since 1992, he has worked MMIC circuits operating at W-band frequencies and higher. He currently supports numerous research and development programs. Mr. Gorospe was awarded 2012 MWCL “Tatsuo Itoh” Best Paper Award

This article has been accepted for publication in a future issue of this journal, but has not been fully edited. Content may change prior to final publication. Citation information: DOI 10.1109/TTHZ.2021.3083939, IEEE Transactions on Terahertz Science and Technology

X.B. (Gerry) Mei received his B. S degree in Physics from University of Science and Technology of China, in 1987, and his Ph.D degree in electrical engineering from University of California, San Diego in 1997.

He is a Senior Staff Engineer at Northrop Grumman's Micro Electronics Center, leading advanced InP HEMT technology development. He previously worked at Hewlett-Packard/Agilent Technologies as a senior MBE engineer and later an integration engineer. He then worked at Celeritek as a senior member of technical staff, leading the GaAs pHEMT development.

Pekka Kangaslahti (S'94–M'98) received the M.Sc. and Ph.D. degrees from Aalto University (formerly the Helsinki University of Technology), Espoo, Finland, in 1992 and 1999, respectively.

He is a currently Group Supervisor and a Principal Engineer with the Microwave Systems Technology Group, Jet Propulsion Laboratory, California Institute of Technology, Pasadena, CA, USA. His research interests include development of millimeter-wave and submillimeter-wave monolithic microwave integrated circuits, modules, receivers and receiver arrays.

Erich Schlecht (Member, IEEE) received the B.A. degree in astronomy and physics and the M.S. degree in engineering physics from the University of Virginia, Charlottesville, VA, USA, in 1981 and 1987, respectively, and the Ph.D. degree in electrical and computer engineering from The Johns Hopkins University, Baltimore, MD, USA, in 1999.

From 1984 to 1990, he was a Senior Engineer with the National Radio Astronomy Observatory. From 1991 to 1995, he was with Martin Marietta Laboratories, and from 1996 to 1998, he was a Research Assistant with the University of Mary-land at College Park, under contract to the Army Research Laboratory. In 1998, he joined the Jet Propulsion Laboratory (JPL), Pasadena, CA, USA, as a member of the Submillimeter-Wave Advanced Technology (SWAT) team. He is currently Senior Member of the Engineering Staff. His areas of interest are circuit design and Schottky diode modeling for submillimeter wave and terahertz LO frequency multipliers and mixers and astronomical, planetary, and Earth science instruments.

Dr. Schlecht is a member of the IEEE Microwave Theory and Techniques Society (IEEE MTT-S) and the IEEE Antennas and Propagation Society (IEEE AP-S). He has received four NASA technical achievement awards and six new technology invention awards.

Mehmet Ogut received his B.S. degree in electrical and electronics engineering from Bogazici University, Istanbul, Turkey (2007-2011), M.S degree in electrical engineering from the George Washington University, Washington, DC (2011-2013) and Ph.D. degree in electrical engineering from Colorado State University (CSU), Fort Collins, CO, USA (2015-2018).

During his Ph.D. study, he worked on the Tropospheric Water and Cloud Ice (TWICE) small satellite instrument at the Microwave Systems Laboratory (MSL) of CSU as a graduate research assistant. TWICE is a NASA Earth Science Technology Office (ESTO) Instrument Incubator Program (IIP-13) award to develop a millimeter- and sub-millimeter-wave (118 GHz to 670 GHz) radiometer instrument including both window and sounding channels for 6U CubeSat deployment. He focused on the design and testing command and data handling, and power regulation boards, on-orbit reliability analysis of the TWICE instrument including radiation testing and analysis of electrical components, and testing, characterization and calibration of TWICE receivers. In addition, he worked on the deep-learning techniques on the microwave and millimeter-wave radiometry. He applied the deep-learning calibration to High-Frequency Airborne Microwave and Millimeter-wave Radiometer (HAMMR) NASA ESTO IIP-10 project instrument. Currently, he is a technologist in the Microwave Instrument Science Group at the Jet Propulsion Laboratory (JPL), California Institute of Technology, Pasadena, CA. He is the Co-I of Smart Ice Cloud Sensing (SMICES) awarded under NASA ESTO IIP-19 program. His expertise is design, testing, calibration and analysis of microwave and millimeter-wave radiometer instruments, developing innovative concepts in radiometry and artificial intelligence applications in remote sensing.

Dr. Ogut is a member of Eta Kappa Nu, IEEE GRSS and MTTS societies. He was the IEEE R5 ExCom member (2018-2019) and the chair of IEEE High Plains Section Young Professionals Affinity Group (2017-2018). He is currently the Young Professional Ambassador of the IEEE GRSS (2020-2021) and IEEE Rising Stars Organizing Committee member (2019-2021).

Yuriy Goncharenko (Member, IEEE) received the B.S. and M.S. degrees from Kharkov National Polytechnic University, Kharkiv, Ukraine, in 1998 and 1999, respectively, and the Ph.D. degree in radiophysics from the Institute for Radiophysics and Electronics NAS of Ukraine, Kharkiv, in 2006.

From 2012 to 2013, he was a Fulbright Scholar with Applied Physics Laboratory, University of Washington, Seattle, WA, USA, where he focused on airborne synthetic aperture radars for remote sensing of the sea surface. He also

This article has been accepted for publication in a future issue of this journal, but has not been fully edited. Content may change prior to final publication. Citation information: DOI 10.1109/TTHZ.2021.3083939, IEEE Transactions on Terahertz Science and Technology

worked with the University of Birmingham, Birmingham, U.K., on the design of signal processing algorithms for ultraprecise quantum gravity sensors. He is with the Microwave Systems Laboratory, Colorado State University, Fort Collins, CO, USA. His research interests include the design and implementation of calibration, signal processing, and target detection techniques.

Steven C. Reising (S'88–M '98–SM '04) received the B.S.E.E. (magna cum laude) and M.S.E.E. degrees in electrical engineering from Washington University in St. Louis, Saint Louis, MO, USA, and the Ph.D. degree in electrical engineering from Stanford University, Stanford, CA, USA, in 1998.

Since July 2011, he has been a Full Professor in electrical and computer engineering with Colorado State University, Fort Collins, CO, USA, where he was an Associate Professor from 2004 to 2011. Before joining the CSU Faculty in 2004, he was an Assistant Professor in electrical and computer engineering with the University of Massachusetts Amherst, Amherst, MA, USA, from 1998 to 2004, where he received tenure. He was a Summer Faculty Fellow for three years in the Remote Sensing Division, Naval Research Laboratory, Washington, DC, USA. For the first six months of 2014, he was a Visiting Faculty Member of the Sorbonne Universities, University of Paris VI, Université Pierre et Marie Curie, Paris, France. He has been the Principal Investigator of 14Grants from NASA, National Science Foundation (NSF), Department of Defense, Office of Naval Research, Naval Research Laboratory, National Polar-orbiting Operational Environmental Satellite System Integrated Program Office, European Space Agency and Ball Aerospace and Technologies Corporation. He has served as Principal Faculty Advisor for 17 M.S./Ph.D. students who have completed their degrees and are now employed in universities, industry and government laboratories in the U.S., Europe and Asia. His research interests span a broad range of remote sensing disciplines, including microwave remote sensing of the Earth's atmosphere and oceans from airborne platforms, small satellites and CubeSats; radiometer systems from microwave to sub-millimeter-wave and THz frequencies (18-850 GHz); low-noise monolithic microwave integrated circuit design and packaging; lidar systems for sensing temperature and winds in the middle and upper atmosphere; lighting-ionosphere interactions and atmospheric electrodynamics.

Dr. Reising was the recipient of the 2015 George T. Abell Outstanding Research Faculty Award from the College of Engineering at Colorado State University. In 2016, he was the recipient of the Outstanding Service Award from the U.S. National Committee of the International Union of Radio Science (USNC-URSI), presented at the Plenary Session of the 2016 National Radio Science Meeting in Boulder, CO, USA. He was also the recipient of the NSF CAREER Award (2003–2008) in the areas of physical and mesoscale dynamic meteorology, and the Office of Naval Research Young Investigator Program (YIP) Award (2000–2003) for passive microwave remote sensing of the oceans. His Ph.D. student Sharmila Padmanabhan was recipient of the Second Prize Student Paper Award at IGARSS 2003 in Toulouse, France, as well as the URSI Young Scientist Award at the General Assembly in New Delhi, India, in 2005. He won the URSI Young Scientist Award at the General Assembly in Toronto, Canada, in 1999. While at Stanford, he received First Place in the USNC-URSI Student Paper Competition at the 1998 National Radio Science Meeting in Boulder, Colorado. He is the Chair of the Ad-hoc Committee for Intersocietal Relations and as an elected Administrative Committee (AdCom) Member (2003–present) of the IEEE Geoscience and Remote Sensing Society (GRSS). He currently serves as the Vice-Chair of Operations, a member of the Personnel Management Committee and as an elected AdCom Member (2014–present) of the IEEE Microwave Theory and Techniques Society (MTT-S). He previously served as the IEEE MTT-S Inter-Society Committee Chair (2015–2018), IEEE GRSS Vice President of Information Resources (2011–2018), the IEEE GRSS as the Vice President of Technical Activities (2008–2010), an Editor of the GRSS Newsletter (2000–2002) and an Associate Editor for University Profiles (1998–2000). He was a Founding Member of the Editorial Board of the IEEE GEOSCIENCE AND REMOTE SENSING LETTERS (GRSL), with an Impact Factor of 2.9 in 2017, and was an Associate Editor from 2004 to 2013. He has been a Guest Editor of three Special Issues and one Special Section of the IEEE TRANSACTIONS ON GEOSCIENCE AND REMOTE SENSING (TGRS), with an Impact Factor of 4.7 in 2017. He was the U.S. National Committee of the International Union of Radio Science (USNC-URSI) as Immediate Past Chair (2015–2017), the Chair (2012–2014) and a Secretary (2009–2011) of all ten URSI Commissions (ten scientific and technical areas). He was a Secretary of USNC-URSI Commission F (Wave Propagation and Remote Sensing) from 2004 to 2007. He founded and chaired the first three URSI International Student Paper Prize Competitions at the URSI General Assemblies and Scientific Symposia held in Chicago, IL, USA in 2008; Istanbul, Turkey, in 2011; and Beijing, China, in 2014. Prior to that, he chaired the USNC-URSI Student Paper Prize Competition from 2004 to 2008 and at the URSI North American Radio Science Meeting in Ottawa in 2007. In addition, he was a Technical Program Co-Chair for the USNC-URSI National Radio Science Meetings held each January in Boulder, Colorado, from 2010 to 2014. He is a member of URSI Commissions F, G, and H, the American Meteorological Society, the American Geophysical Union, the American Association for the Advancement of Science, Tau Beta Pi and Eta Kappa Nu.

This article has been accepted for publication in a future issue of this journal, but has not been fully edited. Content may change prior to final publication. Citation information: DOI 10.1109/TTHZ.2021.3083939, IEEE Transactions on Terahertz Science and Technology

William R. Deal (M'96–SM'06—F'17) earned his B. S. Degree in Electrical Engineering from University of Virginia in 1996, M.S. and Ph.D. degree from University of California, Los Angeles in 1998 and 2000, respectively. Currently, he is Consulting Engineer at Northrop Grumman's RF Product and Mixed Signal Center in Redondo Beach, CA. He leads a variety of efforts related to developing submillimeter wave technology and inserting submillimeter wave technology into applications. He has authored and co-authored more than 150 journal and conference papers, as well as five book chapters. Dr. Deal received the Outstanding Young Engineer Award in 2009, the 2012 IEEE "Tatsuo Itoh" Best Microwave and Component Letter Paper and the 2016 IEEE Electron Device Letters "George E. Smith" Best Paper Award